

# Wind Engineering Joint Usage/Research Center FY2020 Research Result Report

Research Field: Indoor Environment  
Research Period: FY2020  
Research Number: 20202007  
Research Theme: Research on prediction method of indoor temperature distribution based on mobile sensor information  
Representative Researcher: Weirong Zhang  
Budget [FY2020]: 400000Yen

- \*There is no limitation of the number of pages of this report.
- \*Figures can be included to the report and they can also be colored.
- \*Submitted reports will be uploaded to the JURC Homepage.

## 1. Research Aim

With the increasing requirements of satisfying individual thermal comfort and improving building energy efficiency, the indoor temperature distribution has been attracted more and more attention. Generally, we use Computational Fluid Dynamics (CFD) to obtain the temperature distribution. However, it has the limitation of long calculation time and high calculation load. Additionally, when the thermal boundary conditions change, it is necessary to start repeated calculation. Under this condition, a prediction method of indoor temperature distribution based on the fixed sensor data and the Contribution Ratio of Indoor Climate (CRI) has been proposed. The CRI is an effective index to evaluate the independent contribution of each heat source to temperature distribution.

However, there are some limitations in the location and quantity of temperature data acquisition by using fixed sensors. Therefore, this study proposes to use mobile sensor instead of fixed sensors to obtain discontinuous temperature data in space and time, combined with the CRI, to establish a set of complete, widely used and more accurate prediction model of indoor temperature distribution. This will provide a basis for the coordination and regulation between the air-conditioning terminal systems to improve the efficiency of energy equipment system.

## 2. Research Method

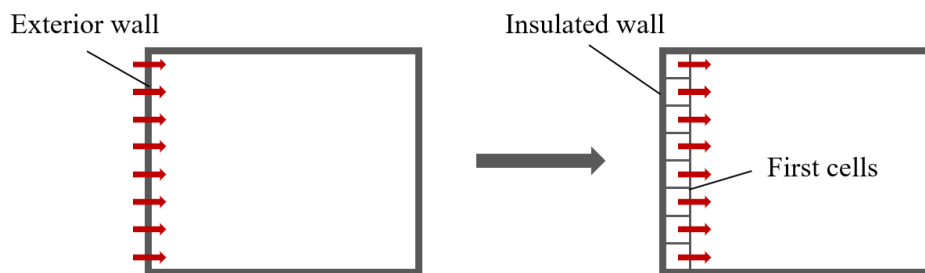
### 2.1 Contribution Ratio of Indoor Climate (CRI)

#### 2.1.1 Positive and negative heat source

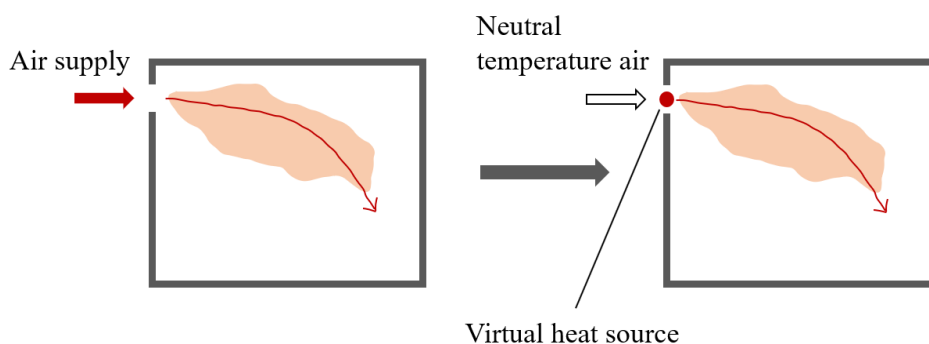
The indoor thermal environment of a building is usually affected by various heat elements, such as heat transfer through walls, solar radiation, and heat emissions from people, lighting and equipment. Although they all have their own heat transfer

properties, they all release heat to or absorb heat from indoor air by means of convection eventually (sometimes after long-wave radiation). In this scenario, all heat elements can be understood in a simple way, i.e., as heat source terms of the energy governing equation. In this study, when a heat source releases heat to indoor air, it is defined as a positive heat source, while when it absorbs heat from indoor air, it is defined as a negative heat source.

Someone may question that why heat transfer through walls and air supply/exhaust from air-conditioning/ventilation, which are usually given as boundary conditions in the energy governing equation, can also be taken as heat sources. In fact, the calculated results are numerically equal, no matter being treated as boundary condition or heat source. For example, as shown in Figure 1(a), the heat transfer through walls can be regarded as convective heat transfer between the indoor air and the first cells next to an adiabatic wall with the same amount of heat transferred. As shown in Figure 1(b), the air supply from an air-conditioning/ventilation system can be separated into two parts, i.e. one is the non-warm/cool air supplied from inlets, and the other is the corresponding positive or negative heat sources that are set at the supply inlets. The non-warm/cool air will be heated or cooled by the positive or negative heat sources to the supply air temperature and then supplied to the room.



(a) Heat transfer through walls as a heat source



(b) Air supply as a heat source

Fig. 1. Models of heat transfer through walls and air supply as heat sources

After identifying all heat sources, a single boundary condition of the whole room or the thermal zone remains, i.e., there is no heat exchange with indoor air.

### 2.1.2 Linear characteristic of temperature field

When all the heat elements of indoor thermal environment are understood as the heat source terms of the energy governing equation, indoor temperature distribution can be regarded as the temporal and spatial synthesis of the influences from all heat sources, as defined by Equation (1),

$$\frac{\partial \theta}{\partial t} + \frac{\partial \theta u_j}{\partial X_j} = \frac{\partial}{\partial X_j} \left( \frac{v_t}{Pr_t} \cdot \frac{\partial \theta}{\partial X_j} \right) + \frac{q}{C_p \rho} \quad (1)$$

Where  $X_j[m]$  is the component of the spatial coordinates ( $j = 1,2,3$ );  $\theta[^\circ C]$  is the air temperature;  $t[s]$  is the time;  $u_j[m/s]$  is the air velocity;  $v_t[kg/(m \cdot s)]$  is the turbulent viscosity;  $Pr_t[J \cdot s]$  is the turbulent Prandtl number;  $q[W]$  is the heat emission and absorption of all heat sources;  $C_p[J/(kg \cdot K)]$  is the specific heat of indoor air;  $\rho[kg/m^3]$  is the air density.

Here, we mainly study the prediction of temperature distribution in the case of forced convection. Generally speaking, the forced convection airflow field is considered as being dominated by the forced convection such as air supply. Although the influences from other heat sources also exist, the effect is smaller than that of forced convection, and thus can be ignored. Therefore, the airflow field can be considered as fixed for a small variation range of supply air temperature and velocity. Under this condition, Equation (1) can be changed into Equation (2),

$$\frac{\partial \theta}{\partial t} + u_j \cdot \frac{\partial \theta}{\partial X_j} = \frac{\partial}{\partial X_j} \left( \frac{v_t}{Pr_t} \cdot \frac{\partial \theta}{\partial X_j} \right) + \frac{q}{C_p \rho} \quad (2)$$

In a fixed airflow field mentioned above, if we can assumed that the buoyancy due to density variations caused by temperature changes can be considered as having little effect on airflow, the indoor temperature field can be assumed to have linear characteristic. In other words, indoor temperature distribution can be expressed by Equation (3), which is the superposition of several sub-temperature fields, each of which is dominated by only one heat source expressed by Equation (4),

$$\frac{\partial \theta}{\partial t} + u_j \cdot \frac{\partial \theta}{\partial X_j} = \frac{\partial}{\partial X_j} \left( \frac{v_t}{Pr_t} \cdot \frac{\partial \theta}{\partial X_j} \right) + \sum_{i=1}^m \frac{q_i}{C_p \rho} \quad (3)$$

$$\frac{\partial \Delta \theta_i}{\partial t} + u_j \cdot \frac{\partial \Delta \theta_i}{\partial X_j} = \frac{\partial}{\partial X_j} \left( \frac{v_t}{Pr_t} \cdot \frac{\partial \Delta \theta_i}{\partial X_j} \right) + \frac{q_i}{C_p \rho} \quad (4)$$

Where  $q_i[W]$  is the heat emission or absorption of heat source  $i$ ;  $\Delta\theta_i[^\circ C]$  is the temperature rise or drop caused by heat source  $i$ .

### 2.1.3 Definition of the CRI

In a forced convection airflow field, the CRI is defined as the ratio of temperature rise or drop at a location caused by one individual heat source to the absolute value of uniform temperature rise or drop caused by the same heat source. It indicates the influence range and degree of each heat source in the fixed airflow field. Its value is a relative intensity, in which the actual temperature rise or drop caused by each heat source is normalized by the absolute value of its own perfect mixing condition. The CRI of the heat source  $i$  at the location  $X_j$  is defined by Equation (5),

$$CRI_i(X_j) = \frac{\Delta\theta_i(X_j)}{\Delta\theta_{i,o}} = \frac{\theta_i(X_j) - \theta_n}{\theta_{i,o} - \theta_n} = \frac{\theta_i(X_j) - \theta_n}{q_i / C_p \rho F} \quad (5)$$

Where  $\theta_n[^\circ C]$  is the neutral temperature, i.e. indoor initial temperature;  $\theta_i(X_j)[^\circ C]$  is the air temperature at the location  $X_j$  caused by heat source  $i$ ;  $\theta_{i,o}[^\circ C]$  is the uniform air temperature caused by heat source  $i$  under the perfect mixing condition;  $\Delta\theta_i(X_j) = \theta_i(X_j) - \theta_n[^\circ C]$  is the temperature rise or drop at the location  $X_j$  caused by heat source  $i$  from  $\theta_n[^\circ C]$ ;  $\Delta\theta_{i,o} = \theta_{i,o} - \theta_n[^\circ C]$  is the uniform temperature rise or drop caused by the heat source  $i$  under the perfect mixing condition from  $\theta_n[^\circ C]$ ;  $F[m^3/s]$  is the volume of supply air.

In an example, the heat emission from the heat source  $i$  is 100W, which results in a temperature rise of 1.5 $^\circ C$  at the location  $X_j$ . If heat diffuses uniformly through the whole space, the uniform temperature rise will be 1 $^\circ C$ . According to Equation (5), the CRI of the heat source  $i$  at the location  $X_j$  is 1.5, indicating that the heat source  $i$  has a greater impact than the average indoor environment at the location  $X_j$ .

## 2.2 A prediction algorithm based on the CRI and finite temperature data

Based on the assumption that the airflow field is fixed, the CRI of each heat source can be seen as constant. That means that if the heat from one heat source increases by a factor of 3, the temperature rise anywhere will increase by a factor of 3. Thus, the CRI

is an effective index to calculate the temperature distribution without the repeated CFD calculation. That is, when the heat from any heat source changes, the temperature change caused by this heat source at any location can be calculated by multiplying the heat by its CRI. A new temperature distribution can then be obtained by superimposing the effect of all heat sources. Therefore, when there are  $m$  heat sources in a room dominated by forced convection, the temperature at any location  $\Delta\theta(X_j)$  is shown in Equation (6),

$$\Delta\theta(X_j) = C_{j1} \cdot \Delta\theta_{1,o} + C_{j2} \cdot \Delta\theta_{2,o} + \dots + C_{jm} \cdot \Delta\theta_{m,o} \quad (6)$$

Where  $C_{ji}$  is the CRI of heat source  $i$  to location  $j$ .

By rewriting Equation (6) into matrix form, Equation (7) is obtained,

$$\Delta\theta(X_j) = \begin{bmatrix} C_{j1} & C_{j2} & \dots & C_{jm} \end{bmatrix} \begin{bmatrix} \Delta\theta_{1,o} \\ \Delta\theta_{2,o} \\ \vdots \\ \Delta\theta_{m,o} \end{bmatrix} \quad (8)$$

However, when predicting the temperature distribution, the intensity of each heat source is not known, that is, the uniform temperature rise or drop caused by it cannot be determined. Therefore, we propose to collect  $n$  temperature data in the space and substitute them into Equation (8) respectively to calculate the uniform temperature rise or drop caused by each heat source, as shown in Equation (9),

$$\begin{bmatrix} \Delta\theta_{s1} \\ \Delta\theta_{s2} \\ \vdots \\ \Delta\theta_{sn} \end{bmatrix} = \begin{bmatrix} C_{11} & C_{12} & \dots & C_{1m} \\ C_{21} & C_{22} & \dots & C_{2m} \\ \vdots & \vdots & \ddots & \vdots \\ C_{m1} & C_{m2} & \dots & C_{mm} \end{bmatrix} \begin{bmatrix} \Delta\theta_{1,o} \\ \Delta\theta_{2,o} \\ \vdots \\ \Delta\theta_{m,o} \end{bmatrix} \quad (9)$$

Where  $\Delta\theta_{si}$  is the temperature rise or drop collected by sensor relative to the neutral temperature. According to Equation (9), in order to calculate  $\Delta\theta_{i,o}$ , we need to multiply the inverse matrix  $C_{ij}$  on the left side of both sides of the equation. This requires that the number of temperature data we collect in space should be equal to the number of heat sources, that is,  $n = m$ . The expression of inverse calculation  $\Delta\theta_{i,o}$  thus obtained is shown in Equation (10),

$$\begin{bmatrix} \Delta\theta_{1,o} \\ \Delta\theta_{2,o} \\ \vdots \\ \Delta\theta_{m,o} \end{bmatrix} = \begin{bmatrix} C_{11} & C_{12} & \dots & C_{1m} \\ C_{21} & C_{22} & \dots & C_{2m} \\ \vdots & \vdots & \ddots & \vdots \\ C_{m1} & C_{m2} & \dots & C_{mm} \end{bmatrix}^{-1} \begin{bmatrix} \Delta\theta_{s1} \\ \Delta\theta_{s2} \\ \vdots \\ \Delta\theta_{sm} \end{bmatrix} \quad (10)$$

Substituting Equation (10) into Equation (8), an expression for predicting the

temperature at any location can be obtained, as shown in Equation (11),

$$\Delta\theta(X_j) = \begin{bmatrix} C_{j1} & C_{j2} & \cdots & C_{jm} \end{bmatrix} \begin{bmatrix} C_{11} & C_{12} & \cdots & C_{1m} \\ C_{21} & C_{22} & \cdots & C_{2m} \\ \vdots & \vdots & \ddots & \vdots \\ C_{1m} & C_{2m} & \cdots & C_{mm} \end{bmatrix}^{-1} \begin{bmatrix} \Delta\theta_{s1} \\ \Delta\theta_{s2} \\ \vdots \\ \Delta\theta_{sm} \end{bmatrix} \quad (11)$$

### 2.3 Mobile sensor experimental platform

Based on the above temperature prediction expression, several fixed sensors have been used to collect the temperature at a fixed location in the space to couple with CRI to predict the temperature at any location. However, there are some limitations in the number and location of fixed sensors. For example, too many fixed sensors are not easy to maintain, and the location of them is far away from the target control area, which leads to the prediction accuracy needs to be improved. Therefore, this study proposes to use mobile sensor instead of fixed sensors to collect temperature data to couple with CRI to predict the temperature distribution. The mobile sensor is shown in Figure 2.



Fig. 2. Mobile sensor

Mobile sensor has the characteristics of flexible acquisition location, variable acquisition height and large amount of data acquisition. We can adjust the acquisition path or height according to need. Additionally, a variety of data combinations can be selected from a large number of the collected data to achieve high-precision prediction of temperature distribution through precision comparison.

### 3. Research Result

To explore the effectiveness of mobile sensor instead of fixed sensors to collect temperature data for temperature distribution prediction, a typical office model as shown in Figure 3 is established and carried out the CFD simulation calculation. There are 10 heat sources, which are lamps, an exterior wall, four people and four computers as one heat source, and there are six groups, five adiabatic walls are regarded as one heat source and air supply. The numerical simulation conditions are shown in Table 1.

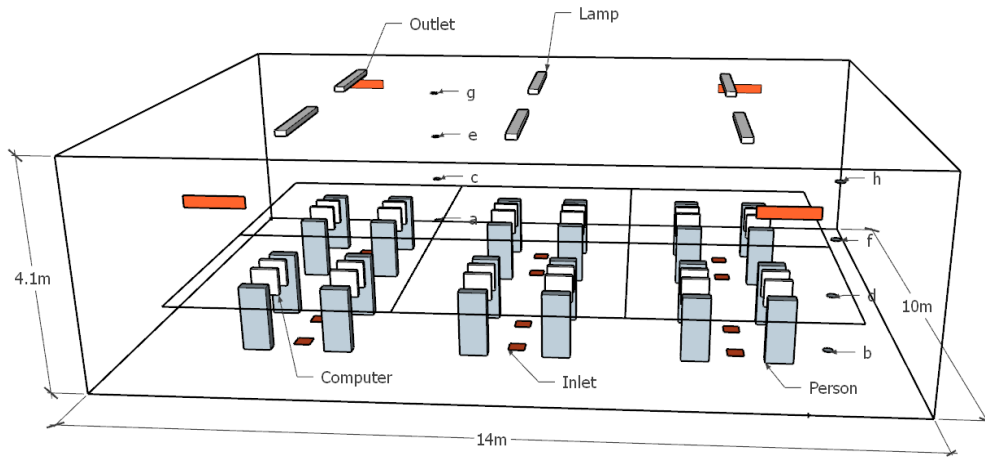


Fig. 3 Room model

Table 1. Summary of numerical simulation

Model	Standard $k-\varepsilon$ model
Mesh	7975777
Air materials	Boussinesq
Boundary conditions	Exterior wall: Heat transfer coefficient $h = 7.2 W / (m^2 \cdot K)$ Outdoor air temperature $T_{out} = 32^\circ C$ Inlet: $v = 0.5 m/s; T = 18^\circ C$ Outlet: outflow Person: Heat flux $q_p = 100W$ Lamp: Heat flux $q_L = 100W$ Computer: Heat flux $q_C = 300W$

In different heights of the office (0.5, 1.5m, 2.5m and 3.5m), two prediction points are set respectively, which horizontal positions are the same, as shown in Figure 3.

The acquisition locations of fixed sensor and mobile sensor are shown in Figure 4. The installation height of the fixed sensor is 3m, and a group of temperature data is collected. The collection height of the mobile sensor is 1.2m, and three groups of temperature data are collected on its moving path (as shown in Figure 3). The temperature of each predicted point calculated by the CFD are considered as their actual temperature.

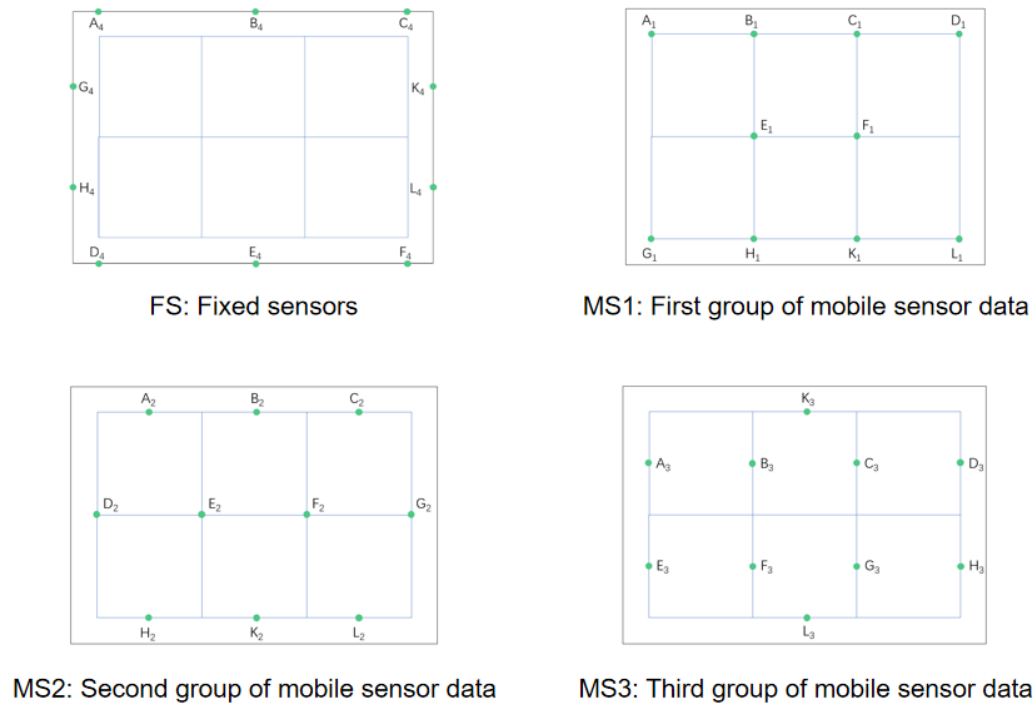


Fig. 4 Acquisition location of sensors

Fig. 5 to Fig. 7 show the comparison of prediction results of the three groups mobile sensor data and the one group fixed sensor data with the actual values. It can be seen from the three pictures that because the installation location is far away from the target area, the prediction accuracy of fixed sensors is lower at the bottom of the room, while the prediction accuracy of using mobile sensor which are closer to the target area is improved. However, above the height of the work area, the prediction accuracy of the mobile sensor is close to that of the fixed sensors. Therefore, we can draw a conclusion that it is feasible to use mobile sensor instead of fixed sensor to predict temperature.

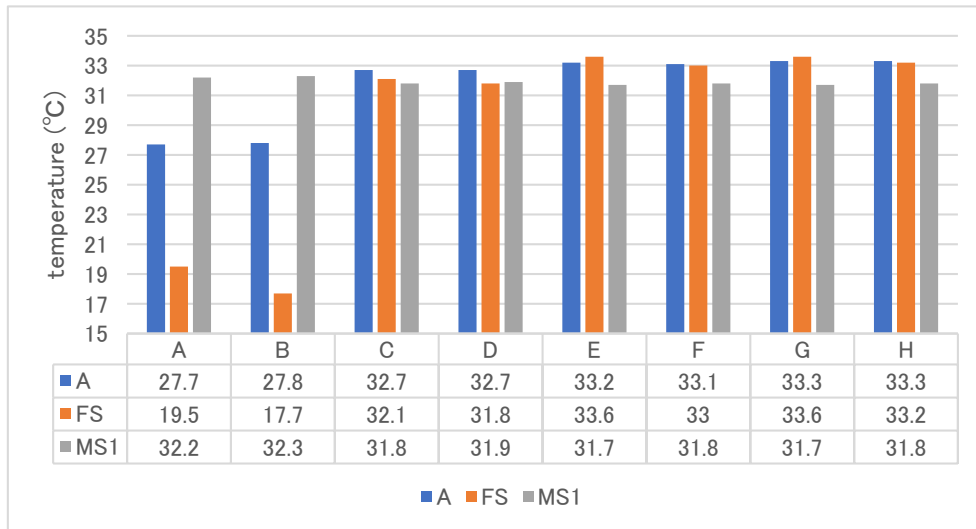


Fig. 5 Comparison of the prediction results of first group of mobile sensor data and fixed sensor with the actual values

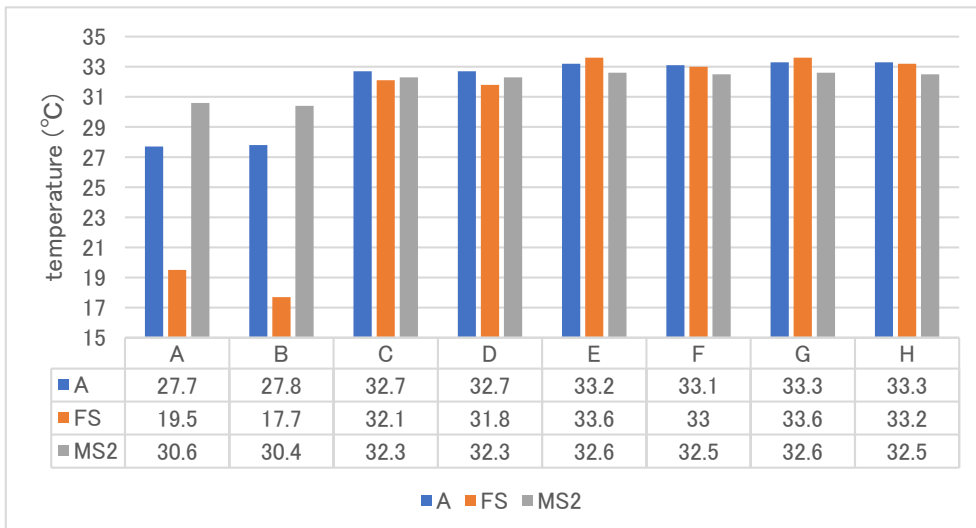


Fig. 6 Comparison of the prediction results of second group of mobile sensor data and fixed sensor with the actual values

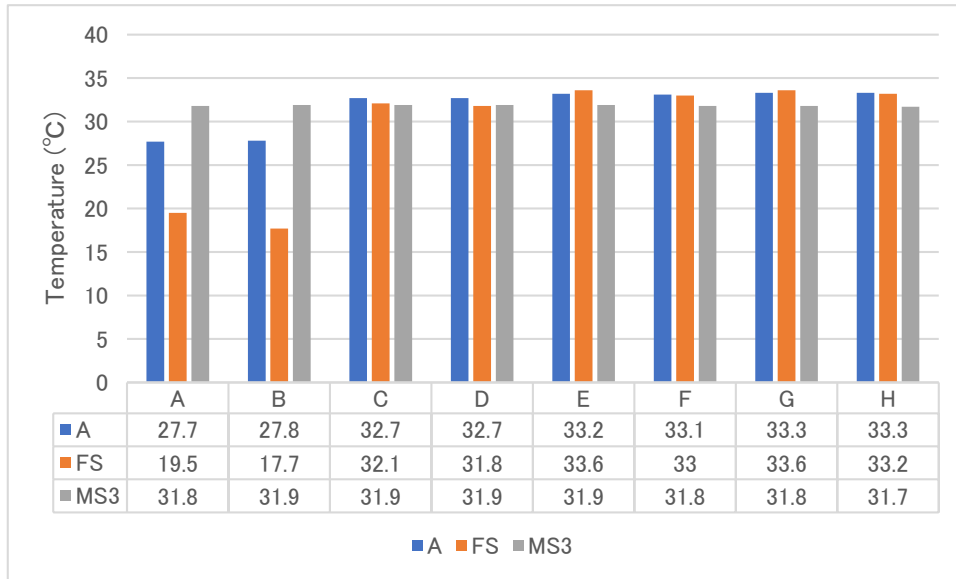


Fig. 7 Comparison of the prediction results of third group of mobile sensor data and fixed sensor with the actual values

Fig. 8 is the comparison of the prediction results of three groups of mobile sensor. Through the accuracy comparison, we can see that there are some differences in the prediction results when selecting different data combinations on the mobile sensor acquisition path. While for areas above the height of the work area, the difference is not obvious.

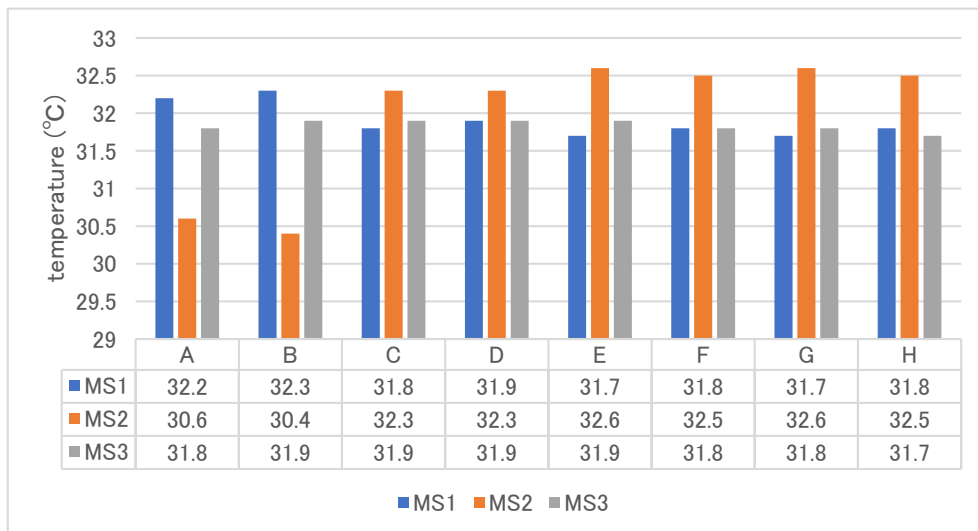


Fig. 8 Comparison of the prediction results of three groups of mobile sensor

For more intuitive error analysis, all calculation results are summarized in Table 2. It can be seen from the table that although the prediction accuracy of the mobile sensor is higher than that of the fixed sensor for the temperature distribution prediction in the bottom of the room, the prediction error is still relatively large. It has the highest accuracy for the temperature prediction prediction near the work area. However, in the area above the height of the work area, the prediction accuracy of the mobile sensor is

even lower than that of the fixed sensor. Therefore, how to design the acquisition height of mobile sensor to achieve more accuracy of temperature distribution prediction needs to be further studied. In addition, through the accuracy analysis, whether the high-precision prediction of the whole space temperature distribution can be achieved through the effective combination of fixed sensor and mobile sensor will also be a direction of our future work.

Table 2. Summary of calculation results

Prediction points	Coordinate (m)	Actual value(°C)	Group 1 (°C)	Group 2 (°C)	Group 3 (°C)	Group 4 (°C)	Average error of mobile sensor (%)	Average error of fixed sensors (%)
A	(4.5, 0.5, 1.5)	27.7	32.2	30.6	31.8	19.5	13.8	29.7
B	(12.5, 0.5, 8.5)	27.8	32.3	30.4	31.9	17.7	13.4	36.3
C	(4.5, 1.5, 1.5)	32.7	31.8	32.3	31.9	32.1	2.0	1.9
D	(12.5, 1.5, 8.5)	32.7	31.9	32.3	31.9	31.8	2.1	2.7
E	(4.5, 2.5, 1.5)	33.2	31.7	32.6	31.9	33.6	3.5	1.1
F	(12.5, 2.5, 8.5)	33.1	31.8	32.5	31.8	33.0	3.4	0.4
G	(4.5, 3.5, 1.5)	33.3	31.7	32.6	31.8	33.6	3.7	1.1
H	(12.5, 3.5, 8.5)	33.3	31.8	32.5	31.7	33.2	3.8	0.2

#### 4. Published Paper etc.

(Underline the representative researcher and collaborate researchers)

[Published papers]

1. Weirong Zhang, Yanan Zhao, Peng Xue, Kunio Mizutani. Review and Development of the Contribution Ratio of Indoor Climate (CRI). Energy and Built Environment (Under review).

[Presentations at academic societies]

- 1.
- 2.

[Published books]

- 1.
- 2.

[Other]

Intellectual property rights, Homepage etc.

#### 5. Research Group

1. Representative Researcher:

Weirong Zhang, Beijing University of Technology, Professor

2. Collaborate researchers:

Kunio Mizutani, Tokyo Polytechnic University, Professor

Yanan Zhao, Beijing University of Technology, Master Student  
Weijia Zhang, Beijing University of Technology, Master Student  
Haotian Zhang, Beijing University of Technology, Master Student  
Zihan Zang, Beijing University of Technology, Master Student

## 6. Abstract (half page)

Research Theme: Research on prediction method of indoor temperature distribution based on mobile sensor information

Representative Researcher (Affiliation): Weirong Zhang (BJUT)

### Summary • Figures

This study explored the effectiveness of using mobile sensor instead of fixed sensors to collect temperature data coupled with the CRI for temperature distribution prediction. Several conclusions can be drawn from this study:

- 1) CRI is an effective index to analyze, built and predict temperature distribution.
- 2) Using the mobile sensor instead of the fixed sensors to predict the temperature distribution is feasible, especially it improves the prediction accuracy of temperature distribution at the bottom of the room.
- 3) Mobile sensor acquisition path, acquisition height and how to select data from the discontinuous data is the focus of future work.
- 4) Whether the high-precision prediction of the whole space temperature distribution can be achieved through the effective combination of fixed sensor and mobile sensor will also be a direction of our future work.

